19th Australasian Tunnelling Conference – Acosta-Martínez, Stewart and Hudson-Smith (Eds.)

Practical shotcrete design approach based on full-scale load-deflection tests using numerical analysis

J. Oh
School of Minerals and Energy Resources Engineering, UNSW Sydney, NSW, Australia

T. Moon
HNTB Corp, New York, NY, USA

ABSTRACT: This study investigates the performance and failure mechanisms of shotcrete in underground construction using numerical analyses by replicating full-scale load-deflection tests based on field test data. A series of parametric studies examined the interaction between support elements such as bolt spacing, shotcrete thickness, and shotcrete bonding under various loading conditions. The analysis results reveal that the ultimate capacity of the shotcrete panel is primarily governed by flexural tensile failure mode after the major bonding failure. The residual bonding area along the periphery of the shotcrete panel plays an important role in reducing the effective moment arm, thereby enhancing the ultimate flexural resistance. In addition, the negative bending moment induced by the interaction between the rock bolt/plate and the shotcrete panel can significantly reduce the positive bending moment at the midspan of the shotcrete panel. Based on these findings, a practical shotcrete design approach using the concept of the bending moment coefficient has been proposed in conjunction with the Q-system.

1 INTRODUCTION

Shotcrete is a crucial method of a ground-support system that is pneumatically sprayed, typically onto the exposed surface of an excavation face, resulting in a compacted, self-supporting, and load-bearing layer. Shotcrete serves as both an essential component of an initial ground support system and the permanent structure, providing a cost-effective application to a variety of civil construction and mining applications. The primary role of shotcrete liners in underground mining or tunnel excavation is to prevent the dilation of loose blocks and ravelling, thereby facilitating the rock fragments to interact with each other (Kaiser & Tannant, 2001).

In general, tensile-flexural failure on a shotcrete liner occurs when the rock fractures and bulges behind the shotcrete layer (Kaiser & Tannant, 2001). Many researchers have devoted considerable efforts to gaining a comprehensive understanding of the various facets of shotcrete failure mechanism and performance. Barrett and McCreath (1995) have attempted to provide shotcrete failure modes for blocky ground conditions, as shown in Figure 1, and postulated a two-step failure process, initially dominated by the loss of adhesion to the rock and followed by flexural failure, and further emphasised that the adhesion is of critical importance in maximising the peak ground support capacity of the shotcrete, whereas flexural strength and toughness play a crucial role in the post-peak behaviour.

The following equations give the proposed design shear and flexural capacity of the shotcrete (Barrett & McCreath, 1995).

$$C_{ds} = 4\tau_{ds}t \quad \text{[kN/m]} \quad \text{For direct shear capacity} \tag{1}$$

$$Mo = \frac{1}{8}w(s-c)^2 \quad \text{[kN-m/m]} \quad \text{For design peak moment} \tag{2}$$

$$C_{flex} = \sigma_{flex}\frac{t^2}{6} \quad \text{[kN-m/m]} \quad \text{For flexural capacity} \tag{3}$$

where t_{ds} is the shear strength of the shotcrete, s is the nominal bolt spacing, t is the thickness of the panel, w is the magnitude of uniformly distributed load, and c is the width of face plates.

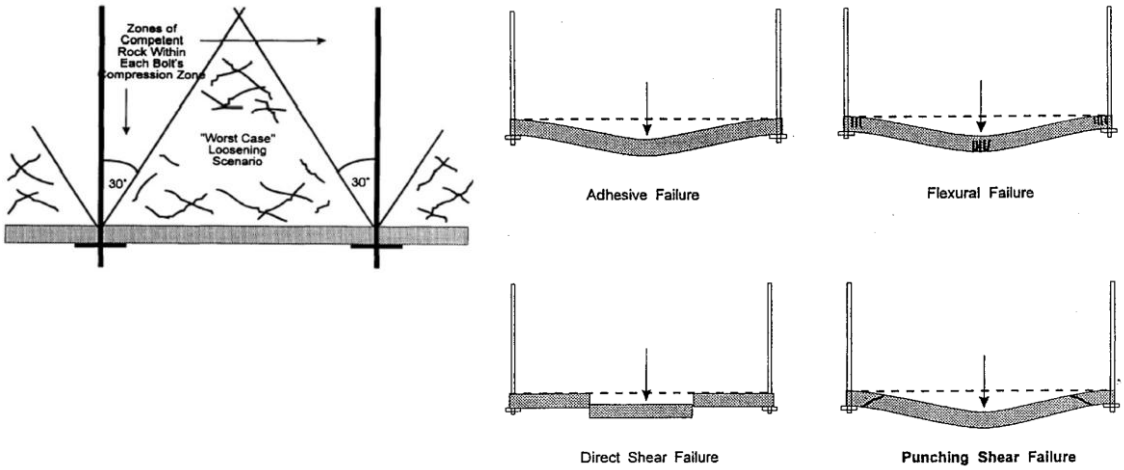

Figure 1. Typical shotcrete failure modes (Barrett & McCreath, 1995)

Although many researchers have elucidated the performance and failure mechanism of the shotcrete liner, unknowns and misinterpretations still remain on the failure process of FRS, such as the interactions between shotcrete and rock bolt configuration, the effect of the shotcrete adhesion, and the effect of in-plane confining loading conditions on the shotcrete liner, etc. These factors are essential in understanding and developing a more practical and suitable shotcrete lining design. Thus, the main objective of the paper is to 1) investigate the influence of those key factors that could affect the performance and the failure mechanism of the FRS using a full-scale load-deflection numerical analysis, 2) identify the influences of bolt spacing and thickness of shotcrete on FRS comparing with the full-scale field tests performed by Forrest (2019) and Bernard et al, 2022, and 3) propose a practical shotcrete design approach based on the findings above.

2 FE MODEL SETUP AND CONFIGURATION

To assess the performance and failure process of the shotcrete panel, a series of numerical analyses have been performed using LS-DYNA, a non-linear three-dimensional numerical software developed by LSTC (2019). The shotcrete panel was modelled with a concrete constitutive model known as the Continuous Surface Cap Constitutive Model (CSCM) (Murray, 2007). This model allows for capturing both the pre- and post-failure behaviour of shotcrete. The influence of fibre reinforcements has been calibrated with tensile fracture energy or strain energy release rate, G_c in the CSCM. The elastic behaviour of the CSCM is governed by the bulk and shear modulus until the yield surface of the CSCM is reached. The yield surface is formulated with three stress invariants and uses a multiplicative formulation to combine a shear failure surface with a hardening compaction cap surface that is smooth and continuous.

The formula of the yield surface shown in Equation (5) is a function of the first, second, and third stress invariants of the deviatoric stress tensor (i.e., J_1, J'_2 and J'_3, respectively), as shown in Equation (4).

$$J_1 = 3P^*, J'_2 = \frac{S_{ij}S_{ij}}{2}, J'_3 = \frac{S_{ij}S_{ik}S_{ki}}{3} \tag{4}$$

$$Y(J_1, J'_2, J'_3, k) = J'_2 - \Re^2 F_f^2 F_c \tag{5}$$

where k is the hardening cap parameter at the intersection of the cap and shear surface, F_f is the shear failure surface, S_{ij} is the deviatoric stress tensor, P^* is pressure, F_c is the hardening cap, and $\Re$ is the Rubin third-invariant factor. The shear failure surface is defined as:

$$F_f(J_1) = \alpha - le^{-\beta J_1} + \theta J_1 \tag{6}$$

where α, β, λ and θ are determined by fitting the model surface to a triaxial compression test for concrete cylinder specimens. The cap hardening surface is defined as:

$$F_c = \begin{cases} 1 - \frac{(J_1 - L(k))^2}{(X(k) - L(k))^2} & for\ J_1 \geq L(k) \\ 1 & for\ J_1 < L(k) \end{cases} \quad (7)$$

$$L(k) = \begin{cases} k & k \geq k_0 \\ k_0 & k \leq k_0 \end{cases}$$

$$X(k) = L(k) + R^* F_f(J_1)$$

Equation 7 describes the cap for the failure surface that occurs when J_1 is greater than or equal to $L(k)$. The value of J_1 at which the shear surface initially intersects with the cap surface is k_0. An increase in $X(k)$ and k signifies the expansion of the cap surface when compaction occurs, while a decrease in $X(k)$ and k signifies a contraction of the cap surface when dilation occurs. This intersection depends upon the cap ellipticity ratio, R^*, which represents the ratio of its major to minor axes. In this manner, compression, shear, and tensile failures are represented and consolidated for post-processing by means of a single damage variable as:

$$\varepsilon_v^P = W\left(1 - e^{D_1(X - X_0) - D_2(X - X_0)^2}\right) \quad (8)$$

where ε_v^P is the plastic volume strain, W is the maximum plastic volume strain, and X_0, R, D_1, and D_2 are model input parameters obtained from the best-fit to pressure-volumetric strain curves in uniaxial compressive strength test. Note that in this study, those input parameters were obtained using the pre-determined default values as a function of compressive strength, shear modulus, and bulk modulus (LSTC, 2019).

To simulate the fracture or crushing of shotcrete in the numerical model, the erosion algorithm, based on Equation (8), is implemented. When the material response in an element reaches a critical value of the plastic strain, the element is immediately deleted. The deletion process is irreversible, meaning that the deleted material will not be able to offer further resistance even when the applied load is reversed. For the sake of the FE model stability, the steel wire mesh embedded in the shotcrete panel was modelled with beam elements based on the elastic constitutive model. In addition, the substrate material in contact with the shotcrete panel was modelled with solid elements using the elastic constitutive model. In this study, coal material was assumed to be the substrate bedrock material, consistent with field test conditions done by Forest (2019). The FE model configuration is shown in Figure 2, and the material properties used in the FE analysis are summarised in Table 1.

The interface between the shotcrete panel and substrate is modelled with the "Surface to Surface Mortar Contact Model" in LS-DYNA. The mortal contact is a penalty-based segment-to-segment contact that incorporates finite element consistent coupling between the non-matching discretisation of the two sliding surfaces (Puso & Laursen, 2004a, b). The contact material properties in this study are assigned with the adhesion strength of 1 MPa and static and dynamic friction coefficients of 0.6 and 0.5, respectively.

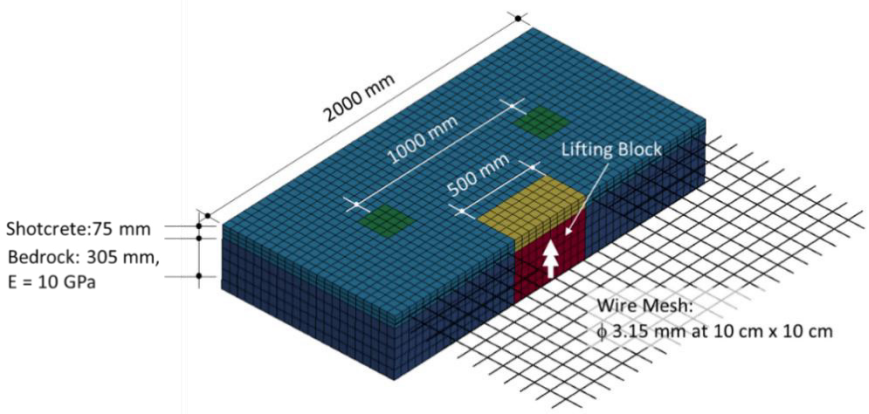

Figure 2. FE model configuration of the full-scale uniformly distributed load-deflection test, spacing-1000 mm, thickness-75 mm.

Table 1. Material properties used in FE analysis

Type	Unit weight (kg/m^3)	Poisson's ratio	f'$_c$ (MPa)	E (GPa)
Shotcrete	2400	0.2	40	30
Steel Wire Mesh	7850	0.3	N/A	215
Substrate rock (Coal)	1500	0.35	N/A	10

2.1 *FE Model calibration*

Before conducting the full-scale load-deflection test, the FE material properties of the shotcrete panel were calibrated based on Uniaxial Compressive Strength (UCS) and Round Panel Tests (RPT) in comparison with the laboratory tests and literature resources (Forrest, 2019, Bernard et al. 2022). It is known that the fibre reinforcements in the shotcrete contribute to an increase in the tensile fracture energy or strain energy release rate, Gc. To calibrate this, various values of Gc were tested, ranging from 75 N-m/m2 to 126 N-m/m2.

The results of UCS tests indicate that despite some minor variation after the peak loads, the maximum UCS of 40 MPa and the Elastic Young's modulus of 30 GPa were found to be constant across the different strain energy release rates. This is attributed to the strain energy release rate, mainly affecting tensile strength.

The RPT has been performed to estimate bending capacity based on ASTM 1550. The FE model configuration of the RPT panel consists of a radius, *R* of 400 mm, thickness, *t* of 75 mm, and the distance between the centre of the support and the centre of the panel, *r*, of 375 mm. The panel is point-supported at the perimeter with a spacing of 120^{o} ° and is loaded by a hemispherical piston at its centre (Bernard & Pircher, 2001). The diameter of the hemispherical loading piston is 50 mm. The loading piston advances at a constant rate of 4.0 mm/min. The interface between the shotcrete panel and the transfer plate is set up with a penalty-based "Surface to Surface Contact Model" in LS-Dyna, while the bottom of the transfer plates is supported by a fixed boundary condition. Table 2 shows the summary of material properties obtained from the laboratory tests and numerical analysis.

Table 2. Material properties obtained from the laboratory tests and numerical analysis

	UCS (MPa)	Adhesive Strength (MPa)	Peak Load of RPT (kN)	Flexural Strength (MPa)
Laboratory Test	44.0	1.0	-	-
Laboratory Test (Forrest, 2019)	44.4	-	23.2 (avg.)	4.5 (avg.)
LS-DYNA (Case 3)	40.0	1.0	22.0	4.2

3 FULL-SCALE LOAD-DEFLECTION TESTS

This section presents the full-scale load-deflection test using numerical analysis, compared with the field test results. A series of sensitivity analyses were performed under various loading conditions to evaluate the influence of shotcrete bonding, shotcrete thickness, and bolt spacing.

3.1 *Full-scale load-deflection field tests*

The full-scale load-deflection field test was conducted in an underground cross-passage in a longwall mine in Australia. The test involved the use of two types of lifting bags, named HLB31 (approximately bag sizes of 500 mm x 500 mm) and V68 (bag size of 1000 mm x 1000 mm), having a maximum load capacity of peak load capacity of 310 kN and 677 kN for HLB31 and V68, respectively. These lifting bags were pre-installed prior to spraying shotcrete. To evaluate

the influence of rock bolt supports, the various spaced M24 JX bolts, Jennmar with the cover plates, were installed, ranging from 1 meter to 2 meters. The length of the bolt is 1.5 meters. After curing the shotcrete liner for around three months, these bags were pressurised with water. Additional details on the field test configuration and procedures can be found in Forrest's thesis (Forest, 2019) and Bernard et al. 2022.

3.2 *Evaluation of shotcrete bonding effect*

The effect of the shotcrete bonding has been investigated using an adhesive strength of 1 MPa obtained from the laboratory tests (Table 2). Due to the lack of information on the adhesion stiffness of the shotcrete, a sensitivity analysis has been performed based on the literature sources (Bae, et al. 2004, Chu & Kwan, 2019, Dong et al. 2016, Saiang et al. 2005). These studies found that the normal bond stiffnesses varied significantly, ranging from 50 GPa/m and 900 GPa/m, depending on the strength of the substrate, roughness of the surface, and adhesion strength, etc.

After conducting a series of trials with various bond stiffnesses, ranging from 54 GPa/m to 540 GPa/m, using the shotcrete sample with 1 meter bolt spacing and a thickness of 75 mm, it has been found that the stiffness of 136 GPa/m is well comparable with the field test results, i.e., maximum bond failure of 106 kN and ultimate load of 210 kN, respectively, as illustrated in Figure 3. In all cases, the first peak loads relating to the initial bonding failure are observed. Afterwards, the resisting loads gradually increase as the deflection increases.

3.3 *Effects of shotcrete bolt spacing and thickness*

The effect of bolt spacings was investigated using 1 m, 1.5 m, and 2 m spacings with a uniform panel thickness of 75 mm. To eliminate the influence of shotcrete bonding, the panel is simply supported by the bolt plates only. Figure 4 illustrates the development of damage/cracking on the shotcrete panel in terms of the load increments. At stage 1, minor damage is initiated at the front face of the panel along the footprint of the push block area, which is likely induced by the flexural damage and/or local shear damage, and other damage at the bottom face is observed near the support plates, which could be associated with the negative bending moment and/or local shear failure induced by the interaction of the bolt plates.

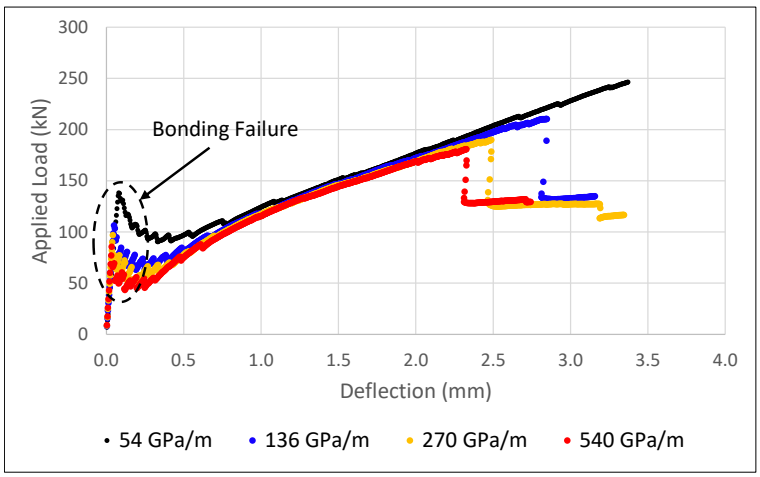

Figure 3. Load-deflection charts estimated from field tests using the scaled peak load in terms of 75 mm thickness.

After this point (a), the deflection is slightly levelled off. As the load increases at stage 2, the damage on the front face of the panel is diagonally extended and propagated, as shown in Figure 4 (b), while the local damage shown on the bottom face extends and interconnects with a round shape. At stage 3, Figure 4 (c), the damage zone further extends, and one of the diagonal damages shown on the right-hand side of the front face asymmetrically propagates further, leading to the panel collapse at Stage 4 (d). Table 5 summarises the analysis results for bolt spacing effects.

Table 2. Summary of analysis results for bolt spacing effects

Bolt Spacing (m)	Panel Thickness (mm)	Max. Deflection (mm)	Max. Resisting Force (kN)
1	75	2.8	169
1.5	75	7.8	135
2	75	12.5	140

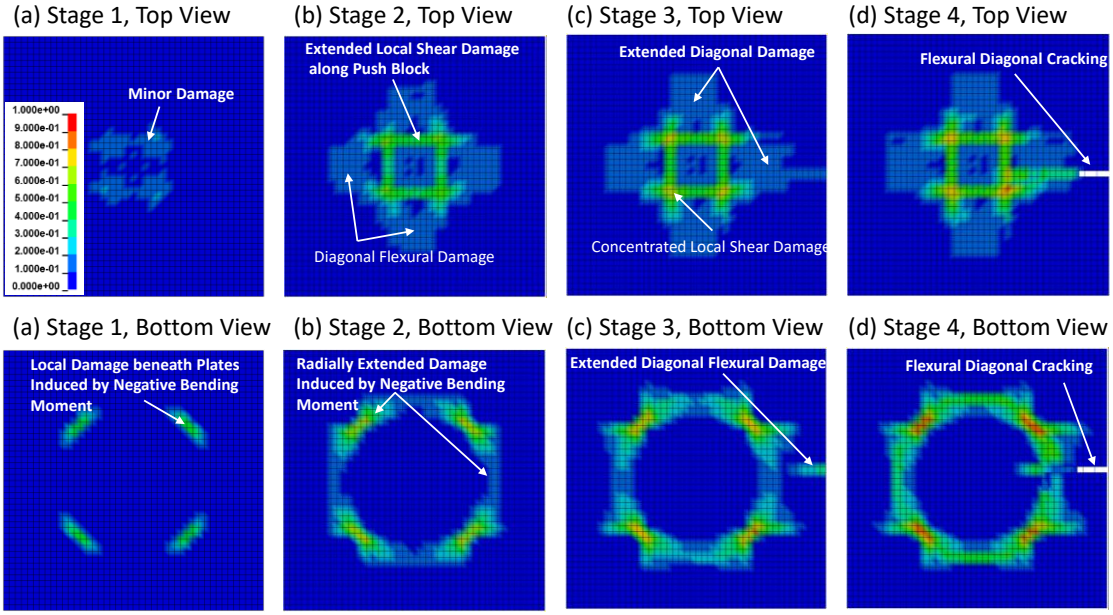

Figure 4. Development of damage distributions and cracking for 1 m bolt spacing without bonding condition.

3.4 *Moment coefficients for shotcrete flexural capacity*

The moment ratio and the corresponding moment coefficient values for all field tests and LS-DYNA analysis results are presented in Figure 5. The field test results for HLB31 and V68, having the shotcrete bonding effect, show a moment ratio of 0.16 and a moment coefficient of 0.02.

A similar result is observed in the LS-DYNA analysis for the shotcrete bond models. These relatively low moment ratio and coefficient values are likely attributed to the bonding effect, which enhances flexural strength. However, in cases where bonding was not considered, the analysis predominantly yielded a moment ratio of 0.2 and a moment coefficient of 0.025. Thus, the ultimate moment induced, M^* representing the ultimate flexural failure of the shotcrete panel, is calculated by the multiplication of M_o and a shown in Equations (9) and (10).

$$M^* = \alpha\left(\frac{1}{8}w(s-c)^2\right) \approx \alpha\frac{P}{8}\ [kN-m/m]$$

$$M^* = 0.16\frac{P}{8} = 0.02P\ [kN-m/m] \quad \text{for bonding condition} \tag{9}$$

$$M^* = 0.2\frac{P}{8} = 0.025P\ [kN-m/m] \quad \text{for no-bonding condition} \tag{10}$$

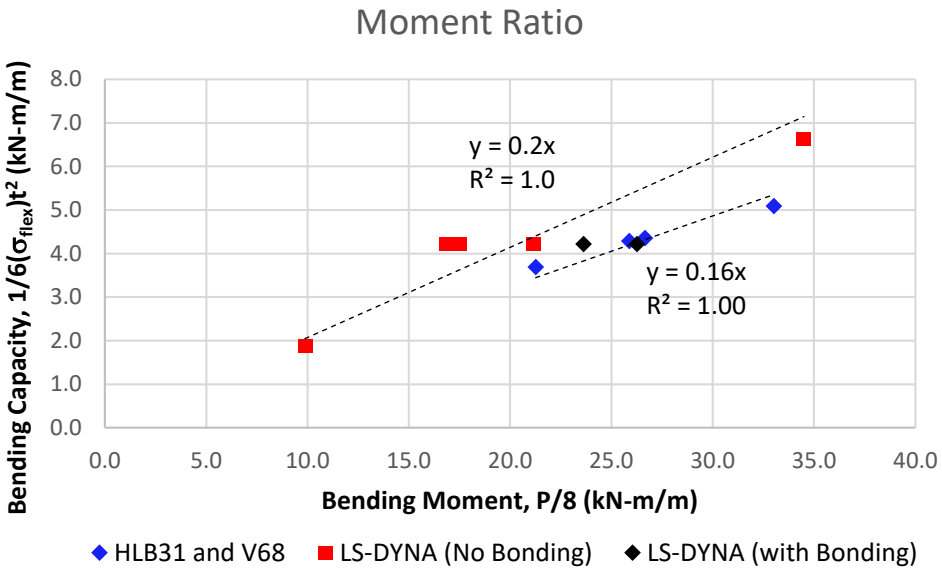

Figure 5. Bending Moment ratios obtained from field tests and LS-DYNA analyses.

4 APPLICATIONS OF SHOTCRETE SUPPORT DESIGN

Using the concept of the moment coefficient mentioned in Section 3.4, a practical shotcrete design approach is proposed in conjunction with the Q-system (Barton et al. 1974). In this shotcrete design approach, the shotcrete adhesion effect is conservatively ignored to take into account the long-term stability and reliable shotcrete design. The critical bending moment acting on the shotcrete panel corresponds to approximately 20 % of the simple span bending moment as formulated in Equation (10).

The ground support pressure, *w* is determined using Eqs 3 and 10, as a function of bolt spacing and shotcrete thickness shown in Equation (11).

$$w = 6.7\sigma_{flex}\left(\frac{t}{s}\right)^2 \quad \text{or} \quad t = 0.39s\sqrt{\frac{w}{\sigma_{flex}}} \tag{11}$$

Subsequently, the ground support pressure is integrated with the Q-system through a generic ground load form, as shown in Equation (12).

$$w = a_1 B\gamma_{rock} Q^{a_2} \tag{12}$$

where a_1 and a_2 represent coefficients, B denotes the tunnel span or height.

The input data points, including tunnel span or height, shotcrete thickness, bolt spacing, and Q values, are retrieved from the Q-system chart (Grimstad & Barton, 1993). For this study, the flexural strength of the shotcrete and rock unit weight are assumed to be 4.5 MPa and 27 kN/m^3, respectively, with the Excavation Support Ratio (ESR) of 1, which represents typical values of design input parameters. The regression analysis yielded the coefficients, a_1 and a_2, of 0.28 and -0.7, respectively, as presented in Equation (13).

$$w = 0.28B\gamma_{rock} Q^{-0.7} \tag{13}$$

For a given bolt spacing, the required shotcrete thickness can be determined using Equations (11) and (13), as follows:

$$t = 0.2s\sqrt{\frac{B\gamma_{rock}Q^{-0.7}}{\sigma_{flex}}} \tag{14}$$

5 CONCLUSION

The main conclusions of this study can be summarised as follows:

- The flexural tensile failure mode predominantly governs the ultimate capacity of the shotcrete liner.
- The effect of shotcrete thickness was evaluated using numerical analysis. The result of the analysis revealed that the maximum resisting loads appear to be a square relation with shotcrete thickness.
- There was a constant ratio between the bending moment capacity, C_{flex} and the estimated bending moment, M_o based on the simple span formula, approximately 0.2 for the "no-bonding condition" and 0.16 for the "bonding condition", respectively.
- A practical shotcrete design method has been proposed based on the moment ratio of 0.2 presented in Equation (11) or Equation (14).

6 REFERENCES

Bae, G.-J., Chang, S.-H., Lee, S.-W., Park, H.-G. (2004). Evaluation of interfacial properties between rock mass and shotcrete. Int. J. Rock Mech. Mining sci. 41, 106-112.

Barrett, S.V.L., McCreath, D.R., 1995, Shotcrete Support Design in Blocky Ground: towards a Deterministic Approach. Tunn. Undergr. space Technol. 10(1), pp. 79-89.

Barton, N., Lien, R., Lunde, J., 1974. Engineering classification of rock masses for the design of tunnel support. NGI Publication No. 106, Oslo, 48.

Bernard, E.S., Oliveira, D.A.F, Forrest, B.H., 2022. In situ flexural failure of unbonded fibre reinforced shotcrete linings in response to point loading, Tunn. Undergr. space Technol. 119, 104235

Bernard, E.S., Pircher, M., 2001, The influence of thickness on performance of fibre-reinforced concrete in a round determinate panel test. Cement, Conc. Aggreg. CCAGDP, 23(1), pp. 23-33.

Chu, S.H., Kwan, A.K.H. (2019). A new bond model for reinforcing bars in steel fibre reinforced concrete. Cement and Concrete Composites, 104, 103405.

Dong, W., Wu, Z., Zhou, X., 2016., Fracture Mechanisms of Rock-Concrete Interface: Experimental and Numerical, 142(7), 1-11.

Forrest, B., 2019. Load capacity of fibre reinforced shotcrete in coal. Master's thesis, UNSW Sydney.

Grimstad, E., Barton, N. 1993. Updating of the Q-system for NMT. Proc. Int. Sym. Sprayed Concrete, Fagerner, Oslo, 22-26, 1993, pp 46-66.

Kaiser, P.K., Tannant, D.D., 2001. The Role of Shotcrete in Hard-Rock Mines. Underground Mining Methods, Engineering Fundamentals and International Case Studies, Hustrulid & Bullock (eds.), Society for Mining, Metallurgy and Engineering Inc., Litteton, CO, pp. 579-592.

LS-DYNA User's Manual Ver R11, 2019. Livermore Software Tech. Corp. Livermore, California.

Murray, Y. 2007, User manual for LS-DYNA concrete material model 159, FHWA-HRT-05-062.

Puso, M.A., Laursen, T.A., 2004a. A mortar segment-to-segment contact method for large deformation solid mechanics. Comput. Methods Appl. Mech. Engrg. 193, pp. 601-629.

Puso, M.A.. Laursen, T.A., 2004b. A mortar segment-to-segment frictional contact method for large deformations, Comput. Methods Appl. Mech. Engrg. 193, pp. 4891-4913.

Saiang, D., Malmgren, L., Nordlund, E. (2005). Laboratory Tests on Shotcrete-Rock Joints in Direct Shear, Tension and Compression. Rock Mech. Rock Eng. 38(4), 275-297.